Journal of Inorganic Biochemistry 141 (2014) 83–93

Contents lists available at ScienceDirect

Journal of Inorganic Biochemistry

journal homepage: www.elsevier.com/locate/jinorgbio

Hydroxyquinoline derived vanadium(IV and V) and copper(II) complexes as potential anti-tuberculosis and anti-tumor agents

Isabel Correia [a,1], Pedro Adão [a,1], Somnath Roy [a,1], Mohamed Wahba [a,f,1], Cristina Matos [a,1], Mannar R. Maurya [b], Fernanda Marques [c], Fernando R. Pavan [d], Clarice Q.F. Leite [d], Fernando Avecilla [e], João Costa Pessoa [a,*,1]

[a] Centro de Química Estrutural, Instituto Superior Técnico, Universidade de Lisboa, Av. Rovisco Pais, 1049-001 Lisboa, Portugal
[b] Department of Chemistry, Indian Institute of Technology Roorkee, Roorkee 247 667, India
[c] Centro de Ciências e Tecnologias Nucleares, Instituto Superior Técnico, Universidade de Lisboa, Estrada Nacional 10,km 139.7, 2695-066 Bobadela LRS, Portugal
[d] Faculdade de Ciências Farmacêuticas, UNESP, C.P. 582, Araraquara, SP 14801-902, Brazil
[e] Departamento de Química Fundamental, Universidade da Coruña, Campus de A Zapateira, 15071 A Coruña, Spain
[f] Inorganic Chemistry Dep., National Research Center, El Buhouth St., Dokki, Cairo, Egypt

ARTICLE INFO

Article history:
Received 8 May 2014
Received in revised form 25 July 2014
Accepted 29 July 2014
Available online 7 August 2014

Keywords:
Vanadium complexes
Copper complexes
Tuberculosis
Cytotoxicity
8-Hydroxyquinoline

ABSTRACT

Several mixed ligand vanadium and copper complexes were synthesized containing 8-hydroxyquinoline (8HQ) and a ligand such as picolinato (pic^-), dipicolinato ($dipic^{2-}$) or a Schiff base. The complexes were characterized by spectroscopic techniques and by single-crystal X-ray diffraction in the case of [$V^{V}O$(L-pheolnaph-im)(5-Cl-8HQ)] and [$V^{V}O(OMe)(8HQ)_2$], which evidenced the distorted octahedral geometry of the complexes. The electronic absorption data showed the presence of strong ligand to metal charge transfer bands, significant solvent effects, and methoxido species in methanol, which was further confirmed by ^{51}V- NMR spectroscopy. The structures of [Cu^{II}(dipic)(8HQ)]Na and [$V^{IV}O$(pic)(8HQ)] were confirmed by EPR spectroscopy, showing only one species in solution. The biological activity of the compounds was assessed through the minimal inhibitory concentration (MIC) of the compounds against *Mycobacterium tuberculosis* (Mtb) and the cytotoxic activity against the cisplatin sensitive/resistant ovarian cells A2780/A2780cisR and the non-tumorigenic HEK cells (IC_{50} values). Almost all tested vanadium complexes were very active against Mtb and the MICs were comparable to, or better than, the MICs of drugs, such as streptomycin. The activity of the complexes against the A2780 cell line was dependent on incubation time presenting IC_{50} values in the 3–14 μM (at 48 h) range. In these conditions, the complexes were significantly ($^{*}P < 0.05$–$^{**}P < 0.001$) more active than cisplatin (22 μM), in the A2780 cells and even surpassing its activity in the cisplatin-resistant cells A2780cisR (2.4–8 μM *vs.* 75.4; $^{**}P < 0.001$). In the non-tumorigenic HEK cells poor selectivity toward cancer cells for most of the complexes was observed, as well as for cisplatin.
© 2014 Elsevier Inc. All rights reserved.

1. Introduction

Tuberculosis is a pulmonary infection disease initiated by the pathogenic bacteria *Mycobacterium tuberculosis* (Mtb) [1]. Despite the development of potentially curative chemotherapy, tuberculosis is responsible for the death of about 2 million people and is still a leading cause of human mortality in the world. In addition, the treatment is expensive, is extended and also causes several side effects and acquired resistance. Therefore many researchers are searching for new alternative compounds for the treatment of tuberculosis, showing minimum inhibitory concentrations (MICs) comparable to, or better than, the reference drugs used in the treatment of this infectious disease [2–4].

Structures derived from biologically active natural products are very important in drug discovery [5]. The 8-hydroxyquinolines (quinolin-8-ols) are known for their antimicrobial properties, among other activities. 8-Hydroxyquinoline (8HQ) itself, is a privileged structure, which is present in many bioactive natural products, and consequently it has been used as a source for many drugs used in a diversity of diseases which include, among many others, neurodegenerative diseases [6,7] and herpes [8]. Di-halogenated 8-hydroxyquinolines are a group of known drugs showing anti-amoebic activity, as well as possessing antibacterial and antifungal properties [9], and were extensively used to treat intestinal infections [10,11]. Namely, clioquinol (5-chloro-7-iodo-quinolin-8-ol = 5-Cl-7-I-8HQ) was widely used to treat diarrhea for around 30 years till the 1970s, and was studied in Phase II trials for Alzheimer's disease [12]. 8HQ has been considered promising for the treatment of tuberculosis [13–15], but to our knowledge it was never used in clinical trials for this purpose.

These antimicrobial properties are considered to be non-selective, and 8HQ derivatives are used topically for antimicrobial action, *e.g.*, anticaries [16]. 8-Hydroxyquinoline has also been commonly used for its chelating ability, especially for Zn^{II} and Cu^{II}[7,17–19]. Cloxyquin (5-chloroquinolin-8-ol = 5-Cl-8HQ) has shown activity against bacteria,

* Corresponding author.
E-mail address: joao.pessoa@ist.utl.pt (J. Costa Pessoa).
[1] Tel.: +351 218419268; fax: +351 218419239.

http://dx.doi.org/10.1016/j.jinorgbio.2014.07.019
0162-0134/© 2014 Elsevier Inc. All rights reserved.

fungi, and protozoa [20–23], and rather recently its anti-tuberculosis activity against Mtb, as well as of many other 8-hydroxyquinolines, including multidrug-resistant strains, was reported [24,14,15]. One of the most potent compounds of this class is 8HQ itself [15].

Substantial progress has been made in the field of tuberculosis research over the last 20 years, which focused mainly on the control of the infection. However, Mtb is still a worldwide health problem, due to the emergence of multi-drug resistant strains of Mtb, and to the association of Mtb and HIV infections, that has caused a global increase in Mtb [25]. First-line drugs for treatment of tuberculosis comprise: isoniazid, rifampin, ethambutol, pyrazinamide and streptomycin [25]. Resistance to these drugs results in treatment failure and the need for application of second-line drugs with a prolonged period of therapy. Even in these cases treatment frequently fails [26,27]. Consequently, there is the need for new anti-tuberculosis agents, especially those with distinct mechanisms of action, so that resistance to the current drugs may be overcome.

Cancer is a class of diseases characterized by unregulated cell growth and represents a major public health problem worldwide [28]. The increase in survival rates is due to better cancer treatment, in particular to more efficient anticancer drugs. Metallo-drugs like cisplatin and its derivatives have been widely used for the treatment of cancer patients; however, these compounds have severe side effects (*e.g.*, nephrotoxicity, toxicity, nausea and vomiting) and acquired resistance. For this reason, there is also much interest in synthesizing new metal compounds, which might be effective for treatment and have less adverse side effects.

Our group has been developing research in the medicinal chemistry field, focusing on the development of transition metal complexes for therapeutic use [29–32], since the application of metal complexes as therapeutic agents is well established, particularly in the anti-cancer field. The anti-microbial activity of vanadium compounds has not been much explored. Namely, only a few studies have been published on vanadium complexes with activity against *M. tuberculosis*[33–35]. Taking this into account, as well as the importance of 8-hydroxyquinolines in medicine, and the fact that metal complexes with drugs may display increased biological activity when compared to the free drugs, we developed vanadium and copper complexes containing 8HQ and other ligands such as picolinic (or dipicolinic) acid or a Schiff base, and investigated their biological activity. Their structural formulae are depicted in Scheme 1. The complexes were fully characterized by spectroscopic methods and X-ray diffraction in selected cases. Their biological activity was assessed through an anti-tuberculosis activity assay (determination of their MICs) and a cancer cell-growth inhibition assay (determination of their IC_{50} values).

2. Experimental

2.1. Materials and methods

All common laboratory chemicals were purchased from commercial sources and used without further purification. Synthesized compounds were characterized by C, H and N elemental analyses, and by FTIR, circular dichroism (CD), ^{1}H, ^{51}V NMR and EPR spectroscopies (whenever appropriate).

2.2. Synthesis of the complexes

2.2.1. $[V^{IV}O(L\text{-pheolnaph-im})]_2$ (**1**)

The precursor compound **1** was prepared by adapting a procedure reported in the literature [36].

2.2.2. $[V^{V}O(naph\text{-}L\text{-}Pheol\text{-}im)(8HQ)]$ (**2**) and $[V^{V}O(naph\text{-}L\text{-}Pheol\text{-}im)(5\text{-}Cl\text{-}8HQ)]$ (**3**)

The procedure for the preparation of compounds **2** and **3** was as follows: 0.40 mmol of the appropriate 8-hydroxyquinoline (0.060 g of 8HQ for **2** or 0.070 g of 5-chloro-8-hydroxyquinoline for **3**) was added to a tetrahydrofuran (THF) solution (20 mL) of complex **1** (0.15 g, 0.40 mmol). The mixture was stirred for 24 h at room temperature and 100 mL of water was then added to the dark red mixture obtained. The precipitate was filtered, washed with water and *n*-hexane and dried under vacuum.

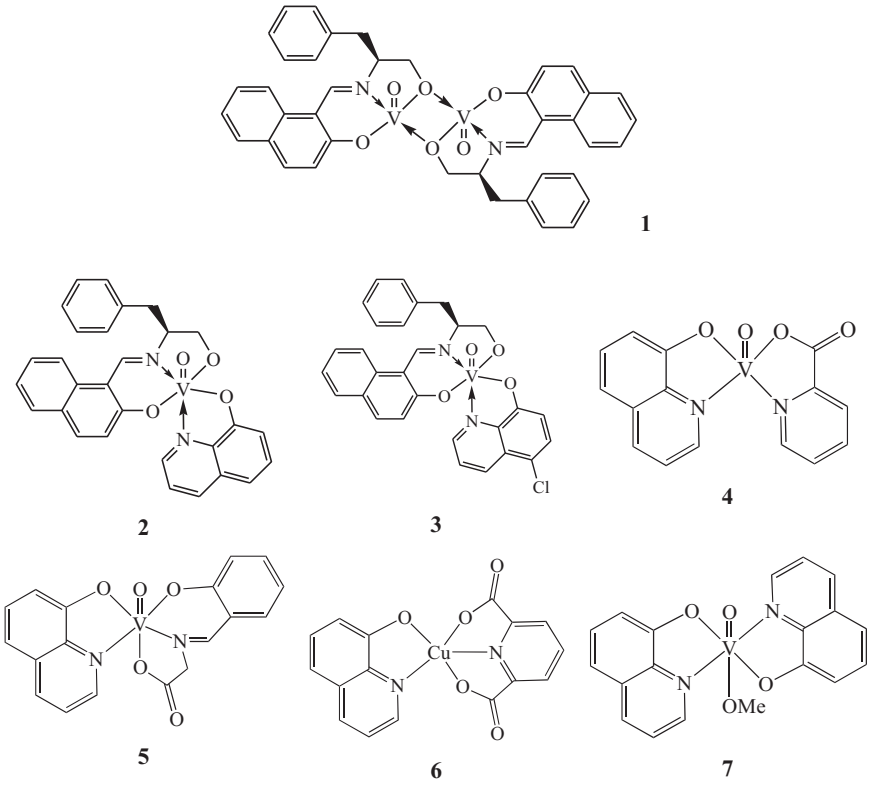

Scheme 1. Schematic molecular structures of some of the compounds prepared and tested in this work.

*2.2.2.1. [$V^{V}O$(L-pheolnaph-im)(8HQ)] (**2**).* Yield: 43% (0.09 g). Elemental analysis calcd. (%) for $C_{29}H_{23}N_2O_4V$: C 67.71, H 4.51, and N 5.45; found: C 68.2, H 4.8, and N 5.1. ^{51}V NMR (300 MHz, $CDCl_3$, δ^{V}/ppm): −493.6 (major) and −482.6 (minor).

*2.2.2.2. [$V^{V}O$(L-pheolnaph-im)(5-Cl-8HQ)] (**3**).* Yield: 64% (0.14 g). Elemental analysis calcd. (%) for $C_{29}H_{22}N_2O_4ClV\cdot 0.5C_6H_{14}$: C 64.93, H 4.94, and N 4.73; found: C 65.0, H 4.4, and N 4.8. ^{51}V NMR (300 MHz, $CDCl_3$, δ^{V}/ppm): −495.6 (major) and −484.6 (minor). Crystals of **3** suitable for single crystal X-ray diffraction were grown from 1,2-dichloroethane solution.

*2.2.3. [$V^{IV}O$(pic)(8HQ)] **4***

10 mL of an ethanolic solution of $V^{IV}O(acac)_2$ (0.53 g, 2.0 mmol) (acac = acetylacetone) and 10 mL of 2-picolinic acid (0.246 g, 2.0 mmol) in ethanol were mixed. The mixture was stirred under nitrogen for 1 h and then 10 mL of 8-hydroxyquinoline (0.29 g, 2.0 mmol) and NaOH (0.08 g, 0.2 mmol) was added. The color of the solution changed from green to brown and precipitation occurred. The brown precipitate was washed with diethyl ether, filtered and dried under vacuum. Elemental analysis calcd. (%) for $C_{15}H_{10}N_2O_4V\cdot 1.2H_2O$: C 50.78, H 3.52, and N 7.90; found: C 50.7, H 3.3, and N 7.7. UV–Vis (λ_{max}/nm and $\varepsilon/M^{-1}\ cm^{-1}$): 271 (9340), 330 (2800), 388 (2500) and 580 (800). FTIR: $\nu(V{=}O) = 964\ cm^{-1}$.

*2.2.4. [$V^{V}O$(Sal-Gly)(8HQ)] **5***

Salicylaldehyde (sal, 0.610 mL, 5.0 mmol) was added to a water solution (10 mL) of glycine (0.375 g, 5.0 mmol) and NaOH (0.40 g, 10 mmol). The mixture was stirred for 1 h, then a solution of $V^{IV}O(acac)_2$ (1.13 g, 5.0 mmol) was added. This mixture was stirred for another hour, followed by addition of 8HQ (0.73 g, 5.0 mmol) and NaOH (0.4 g, 5 mmol) in ethanol. The mixture was stirred for 4 h and the precipitate formed was washed with diethyl ether and ethanol, filtered and dried under vacuum. Elemental analysis calcd. (%) for $C_{18}H_{13}N_2O_5V\cdot 1.5H_2O$: C 52.06, H 3.88, and N 6.75; found: C 52.26, H 3.5, and N 6.6. ^{51}V NMR (DMF, δ^{V}/ppm): −494.1 (100%) and −530.0 (60%). UV–Vis (λ_{max}/nm and $\varepsilon/M^{-1}\ cm^{-1}$): 275 (10920), 319 (4760), 363 (3730) and 570 (1870).

*2.2.5. [Cu^{II}(dipic)(8HQ)]Na **6***

10 mL solution of copper acetate (0.40 g, 2.0 mmol) and 10 mL of dipicolinic acid (0.33 g, 2.0 mmol), both in ethanol, were stirred together for an hour. Then, 10 mL solution of 8HQ (0.29 g, 2 mmol) and NaOH (0.080 g, 2.0 mmol) in ethanol was added. The mixture was stirred for 4 h and the precipitate formed was washed with diethyl ether and ethanol, filtered and dried under vacuum. Elemental analysis calcd. (%) for $C_{16}H_9N_2O_5CuNa\cdot 1.4H_2O$: C 48.28, H 2.99, and N 7.04; found: C 48.3, H 2.7, and N 7.0. UV–Vis (λ_{max}/nm and $\varepsilon/M^{-1}\ cm^{-1}$): 274 (14,000), 340 (1550), 430 (2260) and 770 (45).

*2.2.6. [$V^{V}O(OMe)(8HQ)_2$] **7***

A solution of 8-hydroxyquinoline (0.145 g, 1.0 mmol) in acetone (10 mL) was added to a solution of [$V^{IV}O$(acac)(pydx-aebmz)] (0.48 g, 1.0 mmol), where pydx-aebmz is the Schiff base obtained by condensation of pyridoxal and 2-(2-aminoethyl)-benzimidazole [37], in acetone (40 mL) and stirred for 5 h. The brown color of the solution slowly changed to green. After reducing the volume of the solvent to ca. 15 mL at reduced pressure and keeping at room temperature, a green precipitate was obtained within 24 h. This was filtered out and further dissolved in methanol (10 mL) with heating to give a brown solution. Leaving the solution for slow evaporation in air resulted in brown crystals of [$V^{V}O(OMe)(8HQ)_2$] suitable for X-ray diffraction analysis. Yield: 0.237 g (61%). Using methanol directly gave a brown solution from which a similar brown complex was separated after reducing the solvent volume and keeping at room temperature. Anal. calc. for $C_{19}H_{15}N_2O_4V$: C 59.08, H, 3.91, and N, 7.25%. Found: C, 59.5, H, 3.7, and N, 7.3%. ^{51}V NMR (MeOD-d_4, δ^{V}/ppm): −470.0. UV (λ_{max}/nm): 206, 209, 240, 328, 384 and 504.

2.3. Physicochemical characterization

C, H and N analyses were carried out with a Carlo Erba Model EA1108 elemental analyzer. The FTIR absorption spectra (4000–400 cm^{-1}) of the complexes and the free ligands were measured with KBr pellets with a Bomen FTIR model M102 instrument. The UV-visible (UV–Vis) absorption spectra were measured with a Perkin Elmer Lambda 35 spectrophotometer. ^{51}V NMR spectra of the V^{V}-complexes were recorded on a Bruker Avance III 400 MHz instrument; ^{51}V chemical shifts (δ^{V}) were referenced relative to neat $VOCl_3$ as external standard. The CD spectra were recorded with a JASCO 720 spectropolarimeter with quartz Suprasil® cells. In the 250–700 nm range the usual UV–Vis photomultiplier and 2 to 5 mm path length cells were used, while in the 400–1000 nm range 1, 2 or 5 cm path length quartz cells and a red-sensitive photomultiplier (EXWL-308) as a detector were used.

2.4. Crystallographic study

Crystals suitable for single crystal X-ray diffraction studies of [$V^{V}O$(L-pheolnaph-im)(5-Cl-8HQ)] (**3**) and [$V^{V}O(OMe)(8HQ)_2$] (**7**) were obtained by recrystallization from 1,2-dichloromethane and ethanol, respectively. Three-dimensional X-ray data were collected on a Bruker Kappa Apex CCD diffractometer at low temperature for **3** by the ϕ–ω scan method. Reflections were measured from a hemisphere of data collected from frames each of them covering 0.3° in ω for **3**. Measurements were carried out on an Oxford Xcalibur Gemini, Eos CCD diffractometer with graphite-monochromated CuKα (λ = 1.54178 Å) radiation for **7** and X-ray diffraction intensities were collected (ω scans with ϑ and κ-offsets), integrated and scaled with the CrysAlisPro suite of programs [38]. The unit cell parameters were obtained by least-squares refinement (based on the angular settings for all collected reflections with intensities larger than seven times the standard deviation of measurement errors) using CrysAlisPro for **7**. Data were corrected empirically for absorption employing the multi-scan method implemented in CrysAlisPro for **7**. The structures were solved by direct methods with SHELXS-97 [39] and the molecular model refined by the full-matrix least-squares procedure on F2 with SHELXL-97 [40]. The hydrogen atoms were included in calculated positions and refined with the riding model, except for C(9) and C(10) in **3**, and C(1), C(3), C(5), C(7), C(10), C(11), C(12), C(14) and C(15) in **7**, which were located in a difference Fourier map and left to refine freely. Further details of the crystal structure determinations are given in Table 1. A final difference Fourier map showed no residual density outside: 0.595 and −0.412 $e\cdot Å^{-3}$ for **3** and 0.525 and −0.461 $e\cdot Å^{-3}$ for **7**. A weighting scheme $w = 1/[\sigma^2(F_o^2) + (0.0710P)^2 + 0.00000P]$ for **3** and $w = 1/[\sigma^2(F_o^2) + (0.0515P)^2 + 1.3893P]$ for **7**, where $P = (|F_o|^2 + 2|F_c|^2)/3$, were used in the latter stages of refinement. The crystal structure data was deposited as CCDC 1000881 (for **3**) and 812059 (for **7**) and contains the supplementary crystallographic data for the structure reported. The data can be obtained free of charge *via*http://www.ccdc.cam.ac.uk/conts/retrieving.html, or from the Cambridge Crystallographic Data Centre, 12 Union Road, Cambridge CB2 1EZ, UK; fax: (+44) 1223 336 033; or e-mail: deposit@ccdc.cam.ac.uk.

2.5. Anti-M. tuberculosis activity assay

The anti-Mtb activity of some of the ligands and of the vanadium complexes was determined by the Resazurin Microtiter Assay (REMA) [41]. Stock solutions of the compounds were prepared in DMSO and diluted in Middlebrook 7H9 broth (Difco Laboratories), supplemented with oleic acid, albumin, dextrose and catalase (OADC enrichment

Table 1
Crystal and structure refinement data for **3** and **7**.

Formula	$C_{31}H_{26}Cl_3N_2O_4V$ (**3**)	$C_{19}H_{15}N_2O_4V$ (**7**)
Mr	647.83	386.27
T [K]	100(2)	153.2
λ, Å [Mo, Kα]	0.71073	0.71073
Crystal system	Monoclinic	Monoclinic
Space group	$P2_1$	$P2_1/c$
a [Å]	10.6045(5)	13.982(3)
b [Å]	11.4552(6)	7.8774(16)
c [Å]	12.0644(7)	15.497(3)
β [°]	104.058(3)	109.84(3)
Z	2	4
Volume [Å^3]	1421.65(13)	1605.6(6)
D_{calcd}[g/cm^{-3}]	1.513	1.598
μ mm^{-1}	0.672	0.647
Reflections measured	17,791	14,758
Independent reflections[a]	5576	2389
R(int)	0.0557	0.0576
Goodness-of-fit on F^2	1.032	1.001
R_1[b]	0.0478	0.0438
wR_2 (all data)[b]	0.1321	0.1197

[a] $I > 2\sigma(I)$.
[b] $R_1 = \sum||F_o| - |F_c|| / \sum|F_o|$ and $wR_2 = \{\sum[w(|F_o|^2 - |F_c|^2)^2] / \sum[w(F_o^4)]\}^{1/2}$.

BBL/Becton Dickinson, Sparks, MD, USA), to obtain final drug concentration ranges from 0.15 to 250 μg/mL. The serial dilutions were carried out with a Precision XS Microplate Sample Processor (BioTek™). The isoniazid was dissolved in distilled water, according to the recommendations of the manufacturer (Difco Laboratories, Detroit, MI, USA), and used as a positive control. *M. tuberculosis* H37Rv ATCC 27294 was grown for 7–10 days in Middlebrook 7H9 broth supplemented with OADC, plus 0.05% Tween 80 to avoid clumps.

Suspensions were prepared and their turbidities matched to the optical density of the McFarland no. 1 standard. After a further dilution of 1:25 in Middlebrook 7H9 broth supplemented with OADC, 100 μL of the culture was transferred to each well of the 96-well microtiter plate (NUNC), together with the test compounds. Each assay was set up in triplicate. Microplates were incubated for 7 days at 37 °C, and then resazurin was added for the reading after 24 h of incubation in the same conditions. The wells that turned from blue to pink, with the development of fluorescence, indicated growth of bacterial cells, while maintenance of the blue color indicated bacterial inhibition [41,42]. The fluorescence was read (530 nm excitation filter and 590 nm emission filter) in a SPECTRAfluor Plus (Tecan) microfluorimeter. As positive control the MIC of isoniazid was determined on each microplate. The acceptable range of isoniazid MIC value is 0.015–0.05 μg/mL [41,42].

2.6. Anti-tumor activity

2.6.1. Cell culture conditions

The human ovarian adenocarcinoma cells, A2780 (cisplatin sensitive) and A2780cisR (cisplatin resistant) and a non-tumorigenic cell line, the human embryonic kidney cells HEK-293 (American Type Culture Collection, ATCC) were used in this study. The cells were maintained in media (Gibco) RPMI 1640 (A2780/A2780cisR) or DMEM (Dulbecco's modified Eagle medium) with Glutamax I (HEK-293) supplemented with 10% (v/v) heat inactivated fetal bovine serum (FBS) and 1% penicillin/streptomycin (Invitrogen). Cell lines were cultured in flasks in a CO_2 incubator (Heraeus, Germany) with 5% CO_2 in a humidified atmosphere at 37 °C. For the assays, cells in exponential growth were detached with trypsin–EDTA, suspended in medium and seeded in 96-well plates at a density of 10^4–2×10^4 cells/200 μL.

2.6.2. Cytotoxicity assays

For evaluation of cellular viability, cells were treated with six concentrations of the compounds within the concentration range 0.1 μM–200 μM previously dissolved in DMSO (final concentration < 1%), diluted in medium and incubated for 24, 48 and 72 h at 37 °C and 5% CO_2. Cisplatin, the positive control for the ovarian cells, whenever applied, was first dissolved in H_2O, then in medium and added at the same concentrations used for the tested compounds. Analysis of cell survival was carried out by the MTT [MTT = 3-(4,5-dimethylthiazol-2-yl)-2,5-diphenyltetrazolium bromide] colorimetric assay at 24, 48 and 72 h of incubation. This assay is based on the reduction of the tetrazolium salt to formazan by a mitochondrial dehydrogenase in metabolic active cells. The cellular viability is proportional to the production of formazan [43]. After each time set for incubation the medium was discarded and a solution of MTT dissolved in phosphate buffered saline (PBS) (0.5 mg/mL) was added to each well (200 μL) and the plates were incubated at 37 °C for 3–4 h. Then, 200 μL of DMSO was added to each well to dissolve the formazan crystals. Absorbance was measured at 570 nm with a plate spectrophotometer (Power Wave Xs, BioTek). Each experiment was repeated at least two times, and each concentration tested in at least six replicates. Results are expressed as a percentage of cellular viability with respect to control wells (cells in the absence of the compounds). The IC_{50} values were calculated from plots for cell survival (%) *versus* compound concentration with the GraphPad Prism software (version 4.0). The anti-tumor activity of the complexes was measured in terms of the IC_{50} (*i.e.*, compound concentration that induces 50% of cell death). The statistical analysis was done using the GraphPad Prism software. $^*P < 0.05$ was considered significant.

3. Results and discussion

The 8-hydroxyquinoline vanadium(IV and V) and copper(II) compounds, synthesized by procedures described in the Experimental section, were obtained in moderate to good yields, and characterized by UV–Vis and FTIR spectroscopy. Schiff base complexes **2** and **3** were obtained by the reaction of the vanadium precursor **1** with the appropriate 8-hydroxyquinoline. Scheme 1 shows the structural formulae of the complexes, which are proposed based on spectroscopic data and elemental analysis. For **3** and **7** crystals suitable for single crystal X-ray diffraction studies were obtained and their structural features are discussed below.

3.1. Single crystal X-ray diffraction studies

Compound **3** consists of the tridentate Schiff base ligand coordinated equatorially to a V^VO^{3+} moiety and the 5-chloro-8-quinolinolato ligand completing the octahedral coordination environment, with a *cis* O_{ArO} and a *trans* N_{pyr}, relative to the V=O bond (Fig. 1). One dichloromethane molecule completes the asymmetric unit. The equatorial plane comprises a [N_{imine}, $O_{phenolate}$, $O_{phenolate}$, O_{RO}] donor atom set (mean deviation from the plane = 0.0343(13) Å), and the V^VO center is projected from this plane by 0.311 Å. This results in a distorted octahedral V^VO center, with strained 5- and 6-membered chelate rings. Selected bond distances and angles are provided in Table 2. The V–N_{imine} bond V(1)–N(1) (2.087(3) Å) is *ca.* 0.2 Å longer than the V–O_{ArO} and V–O_{RO} bonds. The V–N_{pyr} bond V(1)–N(2) (2.375(3) Å) is significantly longer than V(1)–N(1) due to the *trans* effect exerted by the O_{oxido} ligand. The V–N_{imine} bond lengths are in line with what was reported for related $V^{IV}O$(Schiff base) compounds [44–48].

Suitable crystals for single crystal X-ray diffraction studies were also obtained for [V^VO(OMe)(8HQ)$_2$] (**7**). The asymmetric unit contains only one molecule of the compound. Nica et al. reported a complex with an identical formulation as a secondary product while reacting ammonium metavanadate with n-hydroxycarbonic acid N-salicylidenehydrazides in the presence of 8HQ [49]. However, although having the same formulation, [V^VO(OMe)(8HQ)$_2$] (**7**) has a different color and the crystals correspond to a distinct asymmetric unit. Crystals of the same compound **7**

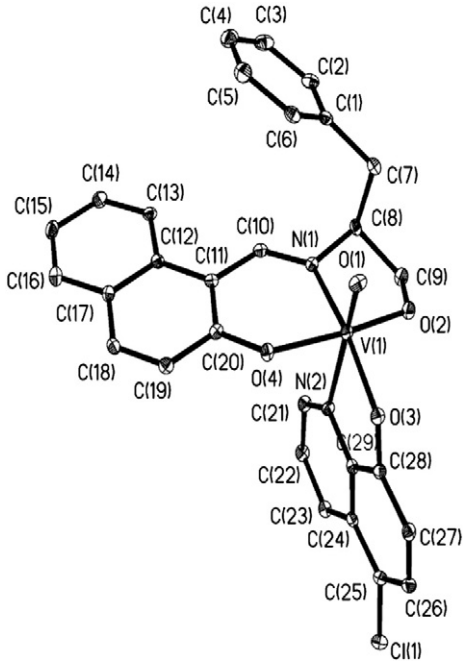

Fig. 1. ORTEP diagram of **3** using 30% probability ellipsoids. Hydrogen atoms are omitted for clarity.

were also obtained from solutions containing complex **5**, and were also characterized by single crystal X-ray diffraction.

This $V^{V}O$-compound **7** presents a distorted octahedral geometry (Fig. 2), with two quinolin-8-olate bidentate ligands with the two N atoms bound *trans* to the O_{oxido} and O_{MeO^-} donors. The bond lengths and angles, Table 2, are in the range found for other related VO-compounds [50,51]. π–π stacking interactions between the aromatic systems are present in the crystal packing with an average distance of *ca.* 3.58 Å.

3.2. Circular dichroism and electronic absorption characterization

Complexes **2** and **3** have chiral Schiff base ligands and were studied by circular dichroism (CD) spectroscopy. The recorded electronic absorption and circular dichroism spectra are shown in Figs. 3 and 4. The relevant λ_{max}, molar absorptivity (ε) and molar circular dichroism (Δε) values obtained for these and for complexes **4**–**6** are listed in Table 3. Spectra were also measured 72 h after sample preparation in order to observe any changes in the spectra with time (Figs. SI-1 to SI-12 and Table SI-1 in Supporting information).

Regarding the electronic absorption spectra of compounds **2** and **3** (Fig. 3), both present very similar band profiles in the same solvent. The most noticeable feature exhibited by both, either in $CHCl_3$ or MeOH, is the strong and broad $O_{phenolate} - V^{V}O$ *pπ–dπ** LMCT bands encompassing the 470–650 nm range. These transitions are typical of phenolate-bound $V^{V}O^{3+}$ species and are also present in the spectrum measured in DMF for **5** [37,52]. A significant solvent effect is also observed. For instance, MeOH causes a decrease in λ_{max} and ε of this LMCT transition relative to $CHCl_3$. A solvent effect is also observed on the azomethine (C═N) *n*–π* and π–π* transitions present in the 360–430 nm range [47,48]. In this case, these transitions are blue-shifted in MeOH and are significantly more prominent and stronger than in $CHCl_3$. The bands below 340 nm are assigned to intraligand transitions. Again, solvent effects manifest in this range similarly as for $\lambda > 350$ nm.

The spectrum measured for the V^{IV}-complex **4** in DMF shows a strong LMCT band due to $O_{phenolate} - V^{IV}O$ *pπ–dπ** transition centered at 580 nm that overlaps the weak d–d transitions. Cu^{II}-complex **6** shows one weak d–d band at 770 nm. These compounds show very low solubility in other solvents and thus solvent effects cannot be evaluated.

Compounds **2** and **3** exhibit CD spectra in the UV and visible range (see Fig. 4). The $O_{phenolato} - V^{V}O$ *pπ–dπ** LMCT transition is present as a very broad positive band encompassing the 500–700 nm range, which in turn indicates the existence of chirality at the metal center [34]. The solvent effect is also observable in this case; this LMCT transition is less intense in MeOH than in $CHCl_3$, although the blue-shift observed earlier is not so discernible. The azomethine (C═N) *n*–π* and π–π* transitions are observed as negative bands in the 350–450 nm range, partly superimposing (and canceling) the charge transfer band in the 450–500 nm range. These transitions have lower associated Δε values in MeOH than in $CHCl_3$. Below 350 nm the CD profiles for compounds **2** and **3** exhibit pronounced solvent effects, which affect the observable λ_{max} of the intraligand transitions, appearing significantly blue-shifted in MeOH relative to $CHCl_3$.

The spectral differences observed may be due to the greater coordinating character of MeOH. Compounds **2** and **3** may partly exchange the alkoxido or quinolinolato ligands for methanol or methoxido ligands. For instance, the exchange of a phenolato donor for a methoxido can explain the decrease in CD intensity of the $O_{phenolato} - V^{V}O$ *pπ–dπ** LMCT transition. Ligand exchange can also occur between the alkoxido donor of the amino alcohol moiety and MeOH, altering the λ_{max} and ε of the CT transitions below 450 nm.

Furthermore, spectral changes were observed 72 h after the preparation of the samples. While the electronic absorption profiles show

Table 2
Selected bond lengths [Å] and angles [°] for **3** and **7**.

Compound **3**				Compound **7**			
Bond lengths/Å				Bond lengths/Å			
V(1)–O(1)	1.603(3)	V(1)–N(1)	2.087(3)	V(1)–O(1)	1.900(2)	V(1)–O(1M)	1.778(2)
V(1)–O(2)	1.830(3)	V(1)–N(2)	2.375(3)	V(1)–O(2)	1.925(2)	V(1)–N(1)	2.296(3)
V(1)–O(3)	1.879(3)	N(1)–C(10)	1.303(5)	V(1)–O(3)	1.594(2)	V(1)–N(2)	2.191(2)
V(1)–O(4)	1.889(3)	N(1)–C(8)	1.478(5)				
Compound **3**				Compound **7**			
Bond angles/°				Bond angles/°			
O(1)–V(1)–O(2)	100.74(13)	O(3)–V(1)–O(4)	96.60(11)	O(3)–V(1)–O(1M)	101.14(10)	O(1M)–V(1)–N(1)	85.45(9)
O(1)–V(1)–O(3)	99.21(12)	O(3)–V(1)–N(1)	159.78(11)	O(3)–V(1)–O(1)	95.80(10)	O(1)–V(1)–N(1)	76.31(9)
O(1)–V(1)–O(4)	96.74(13)	O(3)–V(1)–N(2)	75.74(10)	O(1M)–V(1)–O(1)	101.98(9)	N(2)–V(1)–N(1)	82.97(9)
O(1)–V(1)–N(1)	100.95(13)	O(4)–V(1)–N(1)	82.56(11)	O(3)–V(1)–O(2)	101.02(10)	O(1M)–V(1)–O(2)	91.66(9)
O(2)–V(1)–O(3)	96.07(12)	O(4)–V(1)–N(2)	79.56(11)	O(1)–V(1)–O(2)	155.87(9)	O(3)–V(1)–N(2)	91.61(10)
O(2)–V(1)–O(4)	156.43(12)	N(1)–V(1)–N(2)	84.28(11)	O(1M)–V(1)–N(2)	164.58(9)	O(1)–V(1)–N(2)	85.13(9)
O(2)–V(1)–N(1)	78.72(12)	O(1)–V(1)–N(2)	173.23(13)	O(2)–V(1)–N(2)	77.28(9)	O(3)–V(1)–N(1)	170.73(10)

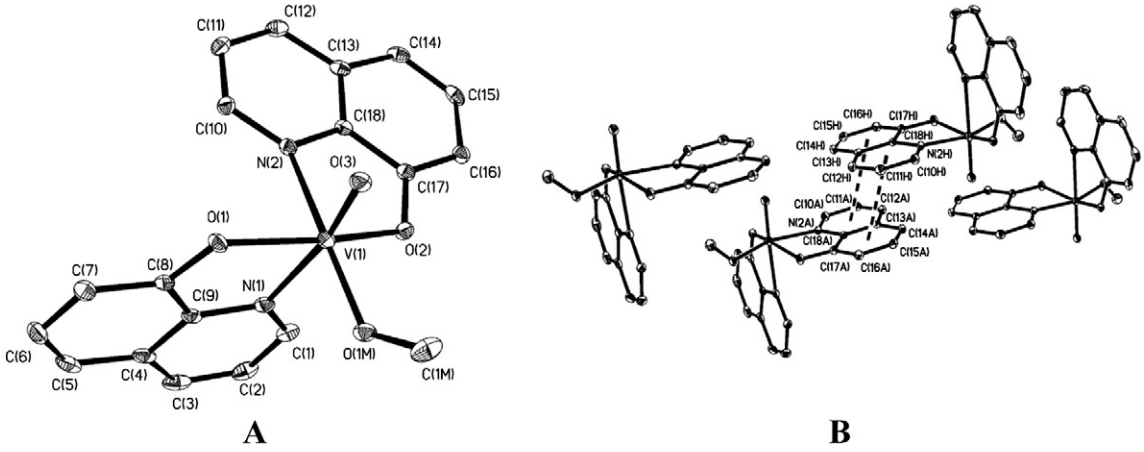

Fig. 2. (A) ORTEP diagram drawn at 30% probability level representing the molecular structure of $[V^{V}O(OMe)(8HQ)_2]$ (**7**), showing the atomic numbering scheme. Hydrogen atoms were omitted for simplicity. (B) Packing view of the crystal structure of $[V^{V}O(OMe)(8HQ)_2]$, where π–π stacking interactions between the aromatic systems are emphasized in the center of the figure.

minor changes with time (see Figs. SI-1 to SI-4 in Supporting information), the CD profiles present a significant overall decrease in optical activity below 450 nm (see Figs. SI-5 to SI-7 in Supporting information). This decrease may be attributed to the partial hydrolysis in solution. In the visible range of the CD spectra the changes after 72 h are much less pronounced or not seen, and this possibly means that the 8HQ ligand, which is responsible for the high intensities of these bands, is still bound to the V^{V} center.

3.3. ^{51}V NMR characterization

All V^{V}-complexes were characterized by ^{51}V NMR spectroscopy and the behavior of compounds **2** and **3** in methanol and chloroform was also compared. The spectra obtained for complexes **2** and **3** are presented in Fig. 5. In $CHCl_3$ they depict very similar spectra, consisting of two observable species within the δ^{V} range: −500 to −480 ppm. It is known that octahedral $V^{V}O$ species coordinated to mixed [N,O] donors may exhibit distinct chemical shifts depending on the donor atoms' *cis*- or *trans*- to the V═O bond [53–56]. In the case of **2** and **3**, the $V^{V}O^{3+}$ center can be coordinated to either a [N_{imine}, O_{RO}, $O_{phenolate}$, $O_{phenolate}$] or a [N_{imine}, O_{RO}, $O_{phenolate}$, N_{pyr}] equatorial donor atom set, each conformational isomer yielding distinct chemical shifts. However, it cannot be predicted which of these isomers is the most stable in solution, despite the crystal structure obtained for **3** indirectly suggesting that it may be the $V^{V}O[N_{imine}, O_{RO}, O_{phenolate}, O_{phenolate}]$-$_{equatorial}$ conformer. The spectrum measured for **5** in DMF depicts two species, the major one at $\delta^{V} = -494.1$ ppm and the minor one at −530.0 ppm. These should correspond to the two conformational isomers, but now the one up-field is less important.

In methanol the ^{51}V NMR spectra of both compounds differ significantly from those in chloroform, with two additional V^{V} species being observed further upfield at $\delta^{V} = -534.8$ ppm and −525.3 ppm (for complex 2, see Fig. 5). The major species observed earlier at *ca.* −494.0 ppm in chloroform is slightly shifted upfield and its intensity is greatly reduced, and the major signals now present are at *ca.* −472 ± 1.5 ppm. These observations suggest the hydrolysis of the Schiff base ligand. Tentatively, the methanol- and methoxido-containing mixed ligand species are assigned to the signals at $\delta^{V} = -534.8$ ppm and −525.3 ppm. Also tentatively, the signals at *ca.* −472 ppm are assigned to either the related V^{V}-complex with one of the O_{oxido} donors protonated [56], *i.e.* to $V^{V}O(OH)$-species, or to a V^{V}-species with a directly coordinated methanol molecule, or $V^{V}O$–8HQ complexes. In fact, complex **7** shows only one peak with $\delta^{V} = -470$ ppm; if we assume that the structure is approximately maintained in solution, the bands with $\delta^{V} \approx -472 \pm 1.5$ ppm, present in the spectra of Fig. 5, may indeed be due to V^{V}–8HQ species.

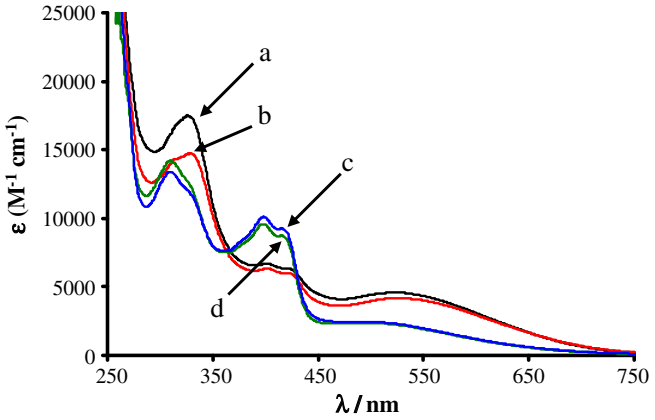

Fig. 3. Isotropic electronic absorption spectra of chloroform and methanol solutions of **2** and **3** measured, with a 1 mm optical path: (a) **2** in $CHCl_3$ (1.2 mM), (b) **3** in $CHCl_3$ (1.3 mM), (c) **2** in MeOH (1.5 mM), and (d) **3** in MeOH (1.4 mM).

3.4. EPR characterization

The paramagnetic complexes **4** and **6** were characterized in solution by EPR spectroscopy. Fig. 6 shows the measured spectra (at 77 K) and those obtained by simulation with the computer program developed by Rockenbauer and Korecz [57].

Both spectra exhibit hyperfine patterns consistent with axial-type spectra of monomeric $V^{IV}O$ and Cu^{II} species. The spin Hamiltonian parameters obtained by simulation were the following: $g_{x,y} = 1.987$, $g_z = 1.951$, $A_{x,y} = 59.7 \times 10^{-4}$ cm^{-1} and $A_z = 169.4 \times 10^{-4}$ cm^{-1} for the $V^{IV}O$-complex **4**, and $g_{x,y} = 2.06$, $g_z = 2.26$, $A_{x,y} = 21 \times 10^{-4}$ cm^{-1} and $A_z = 170.6 \times 10^{-4}$ cm^{-1} for the Cu^{II}-complex **6**.

The values of the $V^{IV}O$ hyperfine coupling constant A_z can be estimated (A_z^{est}) using the additivity relationship [58,59] with an estimated accuracy of $\pm 3 \times 10^{-4}$ cm^{-1}. For complex **4** if we consider a binding mode involving both bidentate ligands in the equatorial plane, and taking $A_z(O_{phenolate}) = 38.9 \times 10^{-4}$ cm^{-1}, $A_z(O_{CO_2}) = 42.6 \times 10^{-4}$ cm^{-1} and $A_z(N_{pyr}) = 44.0 \times 10^{-4}$ cm^{-1}[60,61], then $A_z^{est} = 169.6 \times 10^{-4}$ cm^{-1}, that agrees well with the experimental A_z. For the Cu^{II} complex the ratio $g_z/A_z = 132$ indicates a square pyramidal geometry [62].

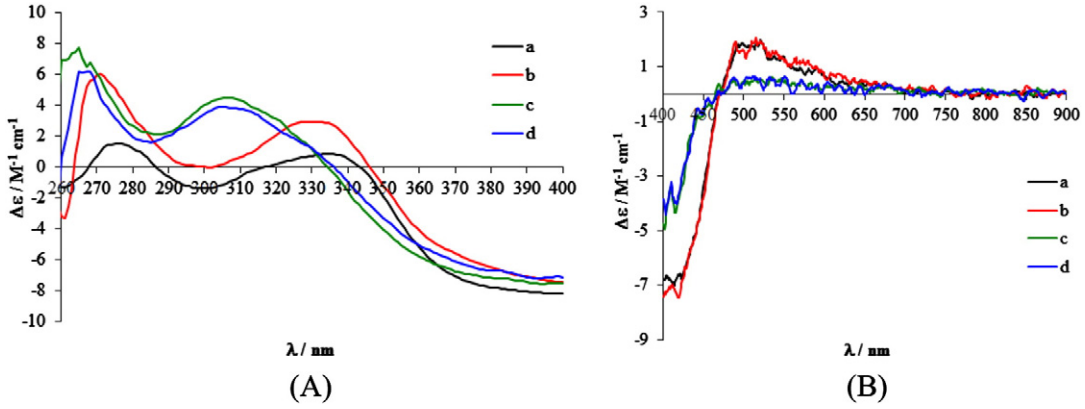

Fig. 4. Circular dichroism spectra of chloroform and methanol solutions of **2** and **3** measured with a 1 mm optical path length: (a) **2** in $CHCl_3$ (1.9 mM), (b) **3** in $CHCl_3$ (1.2 mM), (c) **2** in MeOH (1.5 mM), and (d) **3** in MeOH (1.4 mM).

3.5. Anti-tuberculosis assays

The antibacterial activity of the complexes against the strains of *M. tuberculosis* was evaluated by measuring their MIC values by the REMA Assay [41,42]. The MIC values are included in Table 4; the values for several other complexes were also determined for comparison. The MICs of compounds **2**, **4**, **5** and **7** (*ca.* 1.5 μg/mL) are comparable to, or better than, the MICs of some 'second line' drugs, such as streptomycin (1.0 μg/mL), ciprofloxacin (2.0 μg/mL), p-aminosalicylic acid (0.5–2.0 μg/mL), ethionamide (0.63–1.25 μg/mL), cycloserine (12.5–50 μg/mL), gentamicin (2.0–4.0 μg/mL), ethambutol (0.94–1.88 μg/mL), kanamycin (1.2–5.0 μg/mL), tobramycin (4.0–8.0 μg/mL), clarithromycin (8.0–16 μg/mL) and thiacetazone (0.125–2.0 μg/mL) [15,42,63,64]. If the comparison is made on a molar basis, complexes **2**, **4**, **5** and **7** are more active than all these currently used drugs. In short, some of these complexes are very active against Mtb.

Table 3
Data on electronic transitions of the complexes in solution.

Compound	Solvent	Electronic absorption		Circular dichroism	
		λ/nm	ε/M^{-1} cm^{-1}	λ/nm	Δε/M^{-1} cm^{-1}
2	$CHCl_3$	523	4584	525	1.56
		401	6687	400	−8.21
		326	17,499	334	0.85
				276	1.52
	MeOH	496	2361		
		398	9585	400	−7.55
		310	14,210	306	−4.47
				265	7.74
3	$CHCl_3$	528	4185	515	2.07
		402	6332	400	−7.47
		329	14,746	332	2.94
				271	5.99
	MeOH	491	2448		
		398	10,117	400	−7.14
		310	13,399	305	3.88
				268	6.17
4	DMF	580	800		
		388	2500		
		330	2800		
		271	9340		
5	DMF	570	1870		
		363	3730		
		319	4760		
		275	10,920		
6	DMF	770	45		
		430	2260		
		340	1550		
		274	14,000		

In contrast, complex **3**, containing the cloxyquin ligand, shows no relevant activity (MIC > 25 μg/mL), as well as $V^{IV}O(pic)_2$, $V^{IV}O(dhp)_2$, $V^{IV}O(maltol)_2$, $V^{IV}O(dipic)(H_2O)$ and $Cu(dipic)(H_2O)$. Acetylacetone, $[V^{IV}O(acac)_2]$ and the vanadium salts $V^{IV}OSO_4$ and $NH_4V^{V}O_3$ have not shown any inhibition at the concentration of 50 μg/mL [35], indicating that most probably it is 8HQ that is the relevant species for the activity observed. In fact, 8-hydroxyquinoline was shown to have quite a low MIC [15], and its frequency of resistance (FOR) was estimated to be lower than 10^{-10} [15], which is a significantly better value than the FOR for several currently approved and experimental anti-Mtb drugs [65]; for example, the FOR for rifampicin is ~7×10^{-8} [15].

The ligands being good iron chelators is a factor noticed to be related to good activity against Mtb [66–71]; this is probably related to their ability to bind intracellular iron (or other essential metal ions such as Cu^{II} or Zn^{II}), which is considered essential to the mycobacteria [71]. This would support a non-specific mechanism of action for 8HQ. In fact 8HQ is quite lipophilic and has high affinity for Fe^{III} ($\log \beta_1 = 13$, $\log \beta_2 = 25.3$, $\log \beta_3 = 36.7$ [72]). However, addition of relatively high amounts of iron, copper, zinc or nickel salts had no impact on the MIC determined for 8HQ [15], suggesting that scavenging of essential metals is probably not the main mechanism of action. Additionally, dhp (Deferiprone®) is a well known iron chelator, but we found that $V^{IV}O(dhp)_2$ did not show any relevant activity toward *M. tuberculosis*. It is also known that mycobacteria have a very wide lipid-rich hydrophobic cell wall. Thus, lipophilicity of the compounds and easy penetration into the cell wall are also relevant factors for the activity of the compounds against Mtb. $V^{IV}O(dhp)_2$ is not a particularly lipophilic (or hydrophilic) compound; this may be a factor for its low activity.

Thus, there must be other reasons to explain why 8HQ and complexes **2** and **4**–**7**, containing 8HQ, are very active toward Mtb. Therefore, the knowledge of the molecular basis on how these compounds act in mycobacteria is lacking, as is the case of other compounds such as isoniazid, which is a drug used for a long time in Mtb treatment, for which there is no complete knowledge of its action and resistance in the mycobacteria [73].

The ability of 8HQ to elude resistance suggests interactions with multiple molecular targets. As long as this does not reflect a propensity for host toxicity, it may be a desirable property for anti-infectives, but not much information is available concerning human safety of 8HQ. While high doses of clioquinol (5-Cl-7-I-8HQ) were shown to be neurotoxic in experimental animals, thus probably also in humans, it was argued that the non-halogenated 8HQ would be expected to be less disruptive to membrane potential and could prove safer [15]. The inclusion of 8HQ as ligands in Cu- or V-complexes might theoretically

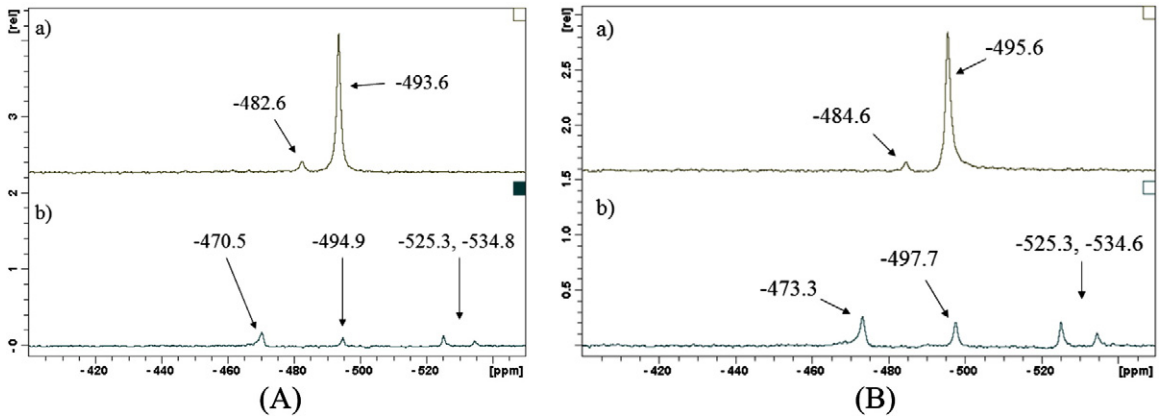

Fig. 5. A) ^{51}V NMR spectra of **2** in $CHCl_3$ (a) and methanol (b). B) ^{51}V NMR spectra of **3** in $CHCl_3$ (a) and methanol (b).

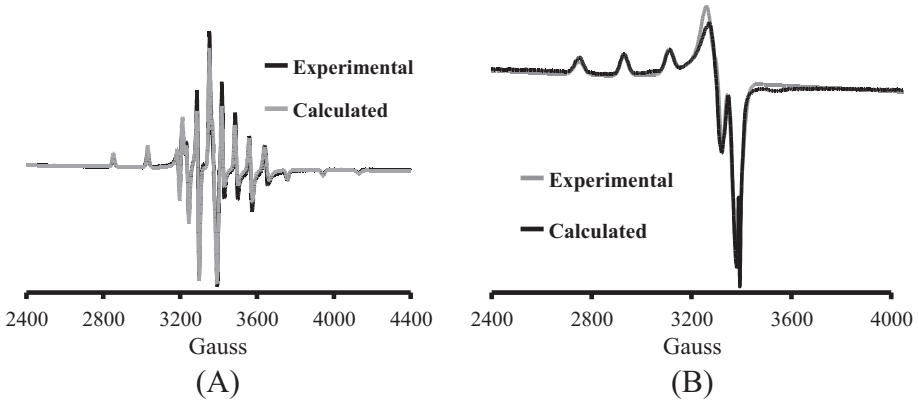

Fig. 6. X-band EPR spectra measured on frozen solutions (77 K) of **4** in DMF (A) and **6** in $CHCl_3$ (B). The calculated spectra obtained by simulation are included for comparison.

improve its bioavailability for use in anti-tuberculosis treatments, but further *in vivo* studies would be required to confirm this possibility.

3.6. Cytotoxicity

The cytotoxic activity of the compounds (complexes and ligands) was evaluated in the A2780 ovarian cisplatin sensitive cells within the concentration range 0.1 μM–200 μM after 24, 48 and 72 h challenge using the colorimetric MTT assay [43]. The IC_{50} values were calculated for each compound and results are presented in Fig. 7 and Table 4 (also in Fig. SI-13 and Table SI-2). Time-dependent cytotoxicity assays with complexes **2**–**7** showed that after 48 h of continuous incubation, the complexes displayed high antiproliferative activities, with IC_{50} values in the micromolar range (3–14 μM). The cytotoxicity of 8HQ, picolinic and dipicolinic acids was also evaluated in the A2780 cells in the same experimental conditions (Fig. 7, Table 4, Table SI-2). The picolinic and dipicolinic acids showed no cytotoxic activity with IC_{50} > 200 μM while 8HQ and cisplatin showed activity with IC_{50} values of 18.8 ± 4.0 μM and 22.4 ± 5.0 μM, respectively. The antiproliferative effect of 8HQ observed in the ovarian tumor cells at longer incubation times could be the result of compound binding to metal enzymes required for DNA synthesis, leading to DNA damage and cell death, although some reports showed that 8HQ had no toxic effects on normal cells (Vero green monkey kidney cells) [7,15].

As shown in Fig. 7, most complexes displayed significantly different cytotoxic activities compared with 8HQ and cisplatin in particular the vanadium complexes **2** (*$P < 0.05$ *vs.* 8HQ and cisplatin), **3** (*$P < 0.05$ *vs.* 8HQ and cisplatin) and **7** (*$P < 0.05$ *vs.* 8HQ and cisplatin) and the copper complex **6** (**$P < 0.001$ *vs.* 8HQ and cisplatin) at 48 h incubation. In the same experimental conditions the IC_{50} value obtained for 8HQ was not significantly different (*ns*) from cisplatin after 48 h treatment.

The cytotoxicity of the compounds against the ovarian cells was also evaluated at 24 and 72 h treatment. After 24 h treatment, the cytotoxic activity of the complexes against A2780 cells is not significantly different

Table 4
Antibacterial activity (MIC) of compounds against strains of *Mycobacterium tuberculosis* and their cytotoxic activity (IC_{50}) against ovarian cancer A2780 cells after 48 h challenge.

Identification	MIC (μg/mL)	MIC (μM)	IC_{50} (μM)
$[V^{V}O$(L-pheolnaph-im)(8HQ)] (**2**)	1.5 ± 2.0	2.9	8.1 ± 2.8
$[V^{V}O$(L-pheolnaph-im)(5-Cl-8HQ)] (**3**)	≥25	≥42.23	5.7 ± 1.6
$V^{IV}O$(pic)(8HQ) (**4**)	1.5 ± 1.3	4.1	14.0 ± 4.5
$V^{IV}O$(sal-Gly)(8HQ) (**5**)	1.4 ± 1.4	3.4	10.9 ± 5.0
Cu^{II}(dipic)(8HQ) (**6**)	–	–	3.1 ± 1.6
$V^{V}O(MeO)(8HQ)_2$(**7**)	1.4 ± 2.2	3.7	5.4 ± 1.9
$Cu(dipic)(H_2O)$	>25	>90	
$V^{IV}O(dipic)(H_2O)$	>25	>90	
$V^{IV}O$(dipic)(phen)	>25	>60	
$V^{IV}O(pic)_2$	>25	>80	
$V^{IV}O(dhp)_2$[a]	>25	>70	
$V^{IV}O(maltol)_2$[a]	>25	>80	
8HQ[b][15]	0.36	2.5	18.8 ± 4.0
Isoniazid [41,42]	0.03	0.22	
Pic	>25		Non-cytotoxic
Dipic	Non-available		Non-cytotoxic

[a] Hdhp = 3-hydroxy-1,2-dimethylpyridin-4(1*H*)-one; Hmaltol = 3-hydroxy-2-methyl-4*H*-pyran-4-one.
[b] We did not find a MIC value for 5-Cl-8HQ; the MIC for 5-Br-8HQ is close to that for 8HQ [15].

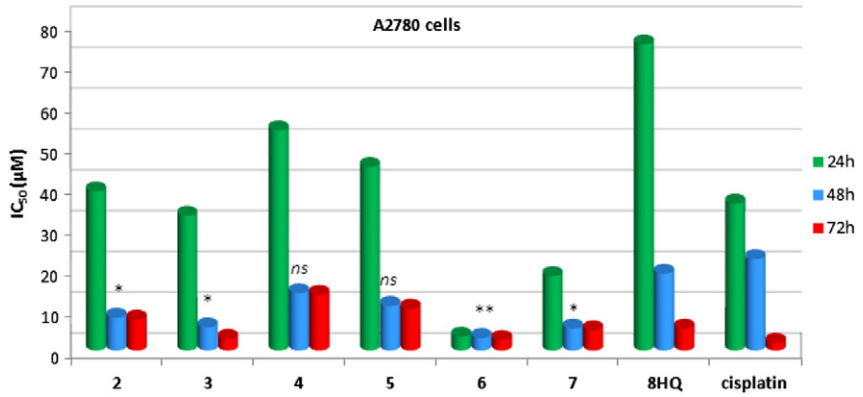

Fig. 7. IC_{50} values found for A2780 ovarian cells after different incubation times with the complexes, 8HQ and cisplatin. The statistical analysis confirmed that the IC_{50} value obtained with 8HQ is not significantly different from cisplatin after 48 h treatment. On the contrary, the IC_{50} values obtained for most of the complexes were significantly different from cisplatin after the same period of incubation: $^{**}P < 0.001$ *vs.* cisplatin for **6**; $^{*}P < 0.05$ *vs.* cisplatin for **2**, **3** and **7** (shown in the figure); not significantly (*ns*) different from cisplatin for **4** and **5**. $^{**}P < 0.001$ *vs.* 8HQ for **6**; $^{*}P < 0.05$ *vs.* HQ for **2**, **3** and **7** at 48 h incubation (not shown in the figure).

from cisplatin (except complex **6**) but significantly different from 8HQ in particular for complexes **2** ($^{*}P < 0.05$ *vs.* 8HQ), **3** ($^{*}P < 0.05$ *vs.* 8HQ) and **7** ($^{**}P < 0.001$ *vs.* 8HQ) and complex **6** ($^{***}P < 0.0001$ *vs.* 8HQ). Copper formed a very active complex with 8HQ, even at short incubation times and, in contrast with the vanadium complexes, the activity did not increase with time of treatment. Results indicated that complexation of 8HQ with the metal ions increased the antiproliferative activities up to 48 h treatment. At 72 h incubation no improvement was observed in complexes' activity, compared to 8HQ and cisplatin.

Compounds' activity was also evaluated in the A2780cisR and non-tumorigenic HEK cells in order to detect any differences between the three cell lines concerning their sensitivity to the compounds and any selectivity with regard to tumor cells. For this purpose, cisplatin, the positive control for the ovarian cancer cells was also included. The results presented in Fig. 8 (also in Table SI-3) demonstrate that all complexes show significantly higher activities (lower IC_{50} values) than cisplatin in the A2780cisR cell line ($^{**}P < 0.001$ *vs.* cisplatin). The activity of the complexes observed in the A2780cisR cell line indicated that complexes can overcome cisplatin cross-resistance in the cisplatin-resistant cell lines, in particular for vanadium complex **4** ($^{*}P < 0.05$, A2780 *vs.* A2780cisR) with a much lower resistance factor (RF) than cisplatin (0.52 *vs.* 3.36) (Table SI-3).

However, in the non-tumorigenic HEK cells the IC_{50} values found for most complexes indicated a not significant selectivity toward cancer cells suggesting that the decrease in cellular viability may be a consequence of toxic effects of the compounds and not due to its anticancer properties. This particularly relates to copper complex **6**, which is the most toxic compound against the three cell lines, with no specific antitumor property. In contrast, complex **7** is a more effective antitumor complex, *i.e.*, showing a significant selectivity against cancer cells. This is an interesting result, i.e., the compound somehow arrests cell proliferation in cancer cells; additionally this is also surpassing cisplatin in the A2780 cisplatin resistant cells, RF = 1.31 *vs.* 3.36 (cisplatin). The analogous complexes **2** ([V^{V}O(naph-L-Pheol-im)(8HQ)]) and **3** [V^{V}O(naph-L-Pheol-im)(5-Cl-8HQ)] appear to present a structure–activity relationship. The presence of chlorine increases the cytotoxic activity in the three cell lines studied after 48 h treatment. This effect was particularly significant in the A2780cisR cells and the HEK cells ($^{*}P < 0.05$, **2** *vs.* **3**).

4. Conclusions

Several 8-hydroxyquinoline derivatives have found application as therapeutic drugs. Taking into account the fact that metal complexes with drugs may display increased or distinct biological activity when compared to the free drug, mixed ligand vanadium(IV and V) complexes [and also copper(II)] containing 8-hydroxyquinoline were synthesized. The complexes were fully characterized by spectroscopic techniques and in some cases by single crystal X-ray diffraction. The crystal structure characterization showed the V^{V}-complexes with distorted octahedral geometry with the 8HQ nitrogen atom coordinated *trans* to the V–oxido bond.

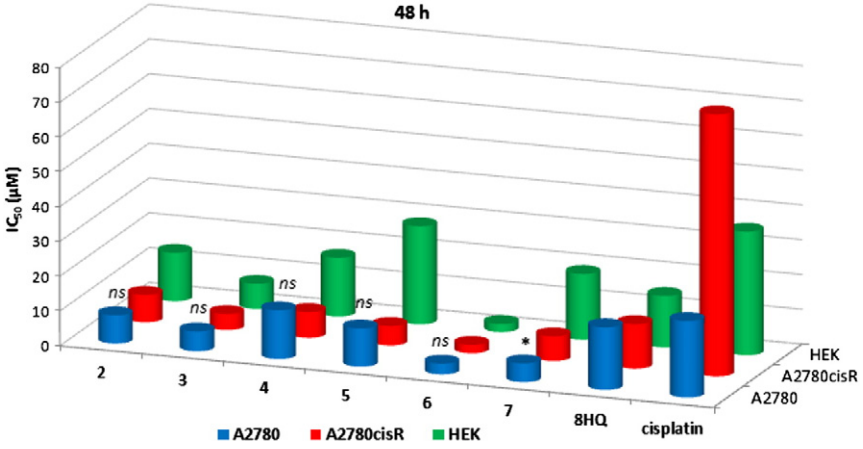

Fig. 8. A comparative evaluation of the IC_{50} values found for A2780/A2780cisR ovarian and HEK cells after 48 h incubation with the compounds and cisplatin. The statistical analysis compares IC_{50} values obtained for the compounds in the A2780 cells *vs.* HEK cells. $^{*}P < 0.05$ for **7** at 48 h treatment. The IC_{50} values obtained with 8HQ, **2**, **3**, **4**, **5** and **6** are not significantly different (*ns*) in both cells after 48 h incubation.

The electronic absorption data showed the presence of strong $O_{phenolate}-V^{V}O$ $p\pi-d\pi^{*}$ LMCT bands, significant solvent effects, and the co-existence of methoxido species in methanol, which was also suggested by ^{51}V NMR spectroscopy. The structure of the Cu^{II} and $V^{IV}O$-complexes was confirmed by EPR spectroscopy, showing the presence of only one species in solution.

The biological activity of the compounds was assessed through the minimal inhibitory concentration of the compounds against *M. tuberculosis* (only for the vanadium complexes) and cytotoxicity to A2780/A2780cisR human ovarian cancer cells (IC_{50} values). Four of the synthesized complexes (**2**, **4**, **5** and **7**) were qualified as potential anti-Mtb agents, having lower MICs than some drugs commonly used to treat Mtb. Interestingly, compound **3**, containing the 5-Cl-8HQ showed no relevant activity. Further *in vivo* studies are required, including the effect against drug-resistant strains and bacilli in a state of latency, as well as to investigate the intramacrophage activity of the new complexes.

The complexes displayed cytotoxic activities in the A2780/A2780cisR ovarian tumor cells, with IC_{50} values ranging from 2.4 to 14 μM after 48 h of continuous treatment and can surpass cisplatin resistance (mainly complex **4**). Complexation of 8HQ with the metal ions improved the antiproliferative activities. This effect seemed to be more evident for shorter incubation times (24 h). The activity of the compounds was also evaluated in the non-tumorigenic HEK cells. Results indicated poor selectivity toward cancer cells for most of the complexes, as well as for cisplatin. Some complexes, particularly complex **7**, $[V^{V}O(OMe)(8HQ)_2]$ are promising dual anti-tuberculosis and antiproliferative metallodrug candidates.

Abbreviations

8HQ	8-hydroxyquinoline
acac	acetylacetone or acetylacetonato
5-Cl-8HQ	5-chloroquinolin-8-ol = cloxyquin
5-Cl-7-I-8HQ	5-chloro-7-iodo-quinolin-8-ol = clioquinol
CD	circular dichroism
DMEM	Dulbecco's modified Eagle medium
DMF	dimethylformamide
FOR	frequency of resistance
HEK cells	human embryonic kidney cells
IC_{50}	compound concentration that induces 50% of cell death
LMCT	ligand to metal charge transfer
MeOH	methanol
MIC	minimum inhibitory concentration
Mtb	*Mycobacterium tuberculosis*
MTT	3-(4,5-dimethylthiazol-2-yl)-2,5-diphenyltetrazolium bromide
ns	not significant
OADC	oleic acid, albumin, dextrose and catalase
N_{imine}	imine-N atom
N_{pyr}	pyridine-N atom
O_{oxido}	oxido-O atom
$O_{phenolate}$	phenolato-O atom
O_{RO}	alcoholato-O atom
PBS	phosphate buffered saline
REMA	Resazurin Microtiter Assay
THF	tetrahydrofuran
δ^{V}	^{51}V chemical shift

Acknowledgments

The authors thank Fundação para a Ciência e a Tecnologia (FCT), the Portuguese NMR and MS Networks (IST Nodes), the Investigador FCT programme, PEst-OE/QUI/UI0100/2013 and São Paulo Research Foundation (FAPESP) for Grant 2013/14957-5.

Appendix A. Supplementary data

Supplementary data associated with this article can be found in the online version, at http://dx.doi.org/10.1016/j.jinorgbio.2014.07.019.

References

[1] A. Zumla, M. Raviglione, R. Hafner, C. Fordham von Reyn, Tuberculosis, N. Engl. J. Med. 368 (2013) 745–755.
[2] F.R. Pavan, G. Von Poelhsitz, F.B. do Nascimento, S.R.A. Leite, A.A. Batista, Victor M. Deflon, Daisy N. Sato, S.G. Franzblau, C.Q.F. Leite, Eur. J. Med. Chem. 45 (2010) 598–601.
[3] F.B. Nascimento, G. Von Poelhsitz, F.R. Pavan, D.N. Sato, C.Q.F. Leite, H.S.S. Araujo, J. Ellena, E.E. Castellano, V.M. Deflon, A.A. Batista, J. Inorg. Biochem. 102 (2008) 1783.
[4] F.R. Pavan, G. Von Poelhsitz, M.I.F. Barbosa, S.R.A. Leite, A.A. Batista, J. Ellena, L.S. Sato, S.G. Franzblau, V. Moreno, D. Gambino, C.Q.F. Leite, Eur. J. Med. Chem. 46 (2011) 5099.
[5] D.A. Horton, G.T. Bourne, M.L. Smythe, Chem. Rev. 103 (2003) 893–930.
[6] P.A. Adlard, R.A. Cherny, D.I. Finkelstein, E. Gautier, E. Robb, M. Cortes, I. Volitakis, X. Liu, J.P. Smith, K. Perez, K. Laughton, Q.X. Li, S.A. Charman, J.A. Nicolazzo, S. Wilkins, K. Deleva, T. Lynch, G. Kok, C.W. Ritchie, R.E. Tanzi, R. Cappai, C.L. Masters, K.J. Barnham, A.I. Bush, Neuron 59 (2008) 43–55.
[7] V. Prachayasittikul, S. Prachayasittikul, S. Ruchirawat, V. Prachayasittikul, Drug Des. Devel. Ther. 7 (2013) 1157–1178.
[8] N.L. Oien, R.J. Brideau, T.A. Hopkins, J.L. Wieber, M.L. Knechtel, J.A. Shelly, R.A. Anstadt, P.A. Wells, R.A. Poorman, A. Huang, V.A. Vaillancourt, T.L. Clayton, J.A. Tucker, M.W. Wathen, Antimicrob. Agents Chemother. 46 (2002) 724–730.
[9] A. Lewis, R.G. Shepherd, Antimycobacterial agents, in: A. Burger (Ed.), Medicinal Chemistry, 3rd ed.John Wiley & Sons, New York, NY, 1970, p. 449.
[10] S.L. Croft, Antiprotozoal agents, in: F. O'Grady, H.P. Lambert, R.G. Finch, D. Greenwood (Eds.), Antibiotic and Chemotherapy: Anti-Infective Agents and Their Use in Therapy, 7th ed.Churchill Livingstone, New York, 1997, pp. 526–527.
[11] E.F. Elslager, Antiamebic agents, in: A. Burger (Ed.), Medicinal Chemistry, 3rd ed. John Wiley & Sons, New York, 1970, pp. 540–541.
[12] C.W. Ritchie, A.I. Bush, A. Mackinnon, et al., Arch. Neurol. 60 (2003) 1685–1691.
[13] F. Tison, Ann. Inst. Pasteur 83 (1952) 275–276.
[14] S. Ananthan, E.R. Faaleolea, R.C. Goldman, J.V. Hobrath, C.D. Kwong, B.E. Laughon, J.A. Maddry, A. Mehta, L. Rasmussen, R.C. Reynolds, J.A. Secrist III, N. Shindo, D.N. Showe, M.I. Sosa, W.J. Suling, E.L. White, Tuberculosis 89 (2009) 334–353.
[15] C.M. Darby, C.F. Nathan, J. Antimicrob. Chemother. 65 (2010) 1424–1427.
[16] D.B. Mirth, A.F. Chite, G.S. Schuster, J. Dent. Res. 57 (1978) 65–71.
[17] M.M. Mashaly, Z.H. Abd-Elwahab, A.A. Faheim, Synth. React. Inorg. Met.-Org. Chem. 34 (2) (2004) 233–268.
[18] E. Sekmo, N. Fukui, Bull. Inst. Chem. Res. 53 (1975) 139–146.
[19] L. Fan, W. Zhu, H. Tian, Synth. Met. 145 (2004) 203–210.
[20] R.F. Cosgrove, S. Baines, Antimicrob. Agents Chemother. 13 (1978) 540–541.
[21] R. Gartner, U. Kaben, Dermatol. Monatsschr. 163 (1977) 711–714.
[22] H. Gershon, M. Gershon, D.D. Clarke, Mycopathologia 158 (2004) 131–135.
[23] K. Grunder, D. Petzoldt, Hautarzt 30 (1979) 392–395.
[24] P. Hongmanee, K. Rukseree, B. Buabut, B. Somsri, P. Palittapongarnpim, Antimicrob. Agents Chemother. 51 (2007) 1105–1106.
[25] S. Ahmad, E. Mokaddas, J. Infect. Public Health 7 (2014) 75–91.
[26] L.G. Dover, G.D. Coxon, J. Med. Chem. 54 (2011) 6157–6165.
[27] M.T. Gutierrez-Lugo, C.A. Bewley, J. Med. Chem. 51 (2008) 2606–2612.
[28] R. Siegel, D. Naishadham, A. Jemal, Cancer statistics, CA Cancer J. Clin. 62 (2012) 10–29.
[29] M. Fernández, J. Varela, I. Correia, E. Birriel, J. Castiglioni, V. Moreno, J. Costa Pessoa, H. Cerecetto, M. González, D. Gambino, Dalton Trans. 42 (2013) 11900–11911.
[30] B. Demoro, R.F.M. Almeida, F. Marques, C.P. Matos, L. Otero, J. Costa Pessoa, I. Santos, A. Rodríguez, V. Moreno, J. Lorenzo, D. Gambino, A.I. Tomaz, Dalton Trans. 42 (2013) 7131–7146.
[31] J. Benítez, A. Cavalcanti de Queiroz, I. Correia, M. Amaral Alves, M.S. Alexandre-Moreira, E.J. Barreiro, L. Moreira Lima, J. Varela, M. González, H. Cerecetto, V. Moreno, J. Costa Pessoa, D. Gambino, Eur. J. Med. Chem. 62 (2013) 20–27.
[32] T. Mukherjee, J. Costa Pessoa, A. Kumar, A.R. Sarkar, Inorg. Chem. 50 (2011) 4349–4361.
[33] A. Maiti, S. Ghosh, J. Inorg. Biochem. 36 (1989) 131–139.
[34] S. David, V. Barros, C. Cruz, R. Delgado, FEMS Microbiol. Lett. 251 (2005) 119–124.
[35] P.I. da, S. Maia, F.R. Pavan, C.Q.F. Leite, S.S. Lemos, G.F. de Sousa, A.A. Batista, O.R. Nascimento, J. Ellena, E.E. Castellano, E. Niquet, V.M. Deflon, Polyhedron 28 (2009) 398–406.
[36] P. Adão, M.L. Kuznetsov, S. Barroso, A.M. Martins, F. Avecilla, J. Costa Pessoa, Inorg. Chem. 51 (2012) 11430–11449.
[37] M.R. Maurya, M. Bisht, N. Chaudhary, A. Kumar, F. Avecilla, J. Costa Pessoa, Eur. J. Inorg. Chem. (2012) 4846–4855.
[38] CrysAlisPro, Oxford Diffraction Ltd., Version 1.171.33.48 (release 15-09-2009 CrysAlis171.NET), 2009.
[39] G.M. Sheldrick, SHELXS-97, Program for Crystal Structure Resolution, Univ. of Göttingen, Göttingen, Germany, 1997.

[40] G.M. Sheldrick, SHELXL-97, Program for Crystal Structures Analysis, Univ. of Göttingen, Göttingen, Germany, 1997.
[41] J.C. Palomino, A. Martin, M. Camacho, H. Guerra, J. Swings, F. Portaela, Antimicrob. Agents Chemother. 46 (2002) 2720–2722.
[42] L.A. Collins, S.G. Franzblau, Antimicrob. Agents Chemother. 41 (1997) 1004–1009.
[43] G. Fotakis, J.A. Timbrell, Toxicol. Lett. 160 (2006) 171–177.
[44] B. Cashin, D. Cunningham, P. Daly, P. McArdle, M. Munroe, N.N. Chonchubhair, Inorg. Chem. 41 (2002) 773–782.
[45] M. Ebel, D. Rehder, Inorg. Chem. 45 (2006) 7083–7090.
[46] I. Correia, J. Costa Pessoa, M.T. Duarte, R.T. Henriques, M.F.M. Piedade, L.F. Veiros, T. Jakusch, T. Kiss, A. Dörnyei, M.M.C.A. Castro, C.F.G.C. Geraldes, F. Avecilla, Chem. Eur. J. 10 (2004) 2301–2317.
[47] J. Costa Pessoa, M.J. Calhorda, I. Cavaco, I. Correia, M.T. Duarte, V. Felix, R.T. Henriques, M.F.M. Piedade, I. Tomaz, J. Chem. Soc. Dalton Trans. (2002) 4407–4415.
[48] I. Cavaco, J. Costa Pessoa, S. Luz, M.T.L. Duarte, P.M. Matias, R.T. Henriques, R.D. Gillard, Polyhedron 14 (1995) 429–439.
[49] S. Nica, A. Buchholz, H. Görls, W. Plass, Acta Crystallogr. E63 (2007) 1450–1452.
[50] I. Cavaco, J. Costa Pessoa, M.T. Duarte, R.T. Henriques, P.M. Matias, R.D. Gillard, J. Chem. Soc. Dalton Trans. (1996) 1989–1996.
[51] I. Cavaco, J. Costa Pessoa, M.T.L. Duarte, P.M. Matias, R.D. Gillard, J. Chem. Soc. Chem. Commun. (1996) 1365–1366.
[52] J.A. Bonadies, C.J. Carrano, J. Am. Chem. Soc. 108 (1986) 4088–4095.
[53] F. Wolff, C. Lorber, R. Choukroun, B. Donnadieu, Inorg. Chem. 42 (2003) 7839–7845.
[54] S. Barroso, P. Adão, F. Madeira, M.T. Duarte, J. Costa Pessoa, A.M. Martins, Inorg. Chem. 49 (2010) 7452–7463.
[55] M.R. Maurya, C. Haldar, A. Kumar, M.L. Kuznetsov, F. Avecilla, J. Costa Pessoa, Dalton Trans. 42 (2013) 11941–11962.
[56] M.R. Maurya, M. Bisht, A. Kumar, M.L. Kuznetsov, F. Avecilla, J. Costa Pessoa, Dalton Trans. 40 (2011) 6968–6983.
[57] A. Rockenbauer, L. Korecz, Appl. Magn. Reson. 10 (1996) 29–43.
[58] K. Wuthrich, Helv. Chim. Acta 48 (1965) 1012–1017.
[59] N.D. Chasteen, in: J. Lawrence, L. Berliner, J. Reuben (Eds.), Biological Magnetic Resonance, vol. 3, Plenum Press, New York, 1981, pp. 53–119.
[60] G. Micera, V.L. Pecoraro, E. Garribba, Inorg. Chem. 48 (2009) 5790–5796.
[61] T. Jakusch, P. Buglyó, A.I. Tomaz, J. Costa Pessoa, T. Kiss, Inorg. Chim. Acta 339 (2002) 119–128.
[62] U. Sakaguchi, A.W. Addison, J. Chem. Soc. Dalton Trans. (1979) 600–608.
[63] D. Sriram, P. Yogeeswari, R. Thirumurugan, Bioorg. Med. Chem. Lett. 14 (2004) 3923–3924.
[64] R.P. Tripathi, N. Tewari, V.K. Dwivedi, Med. Res. Rev. 25 (2005) 93–131.
[65] L.P. de Carvalho, G. Lin, X. Jiang, C. Nathan, J. Med. Chem. 52 (2009) 5789–5792.
[66] S. Floquet, N. Guillou, P. Négrier, E. Rivière, M.L. Boillot, New J. Chem. 30 (2006) 1621–1627.
[67] D.R. Richardson, D.S. Kalinowski, V. Richardson, P.C. Sharpe, D.B. Lovejoy, M. Islam, P.V. Bernhardt, J. Med. Chem. 52 (2009) 1459–1464.
[68] D.R. Richardson, K. Milnes, Blood 89 (1997) 3025–3038.
[69] A. Bacchi, I. Ivanović-Burmazović, G. Pelizzi, K. Andjelković, Inorg. Chim. Acta 313 (2001) 109–119.
[70] K. Andjelković, A. Bacchi, G. Pelizzi, D. Jeremić, I. Ivanović-Burmazović, J. Coord. Chem. 55 (2002) 1385–1392.
[71] G.M. Rodriguez, Trends Microbiol. 14 (2006) 320–327.
[72] T.D. Turnquist, E.B. Sandell, Anal. Chim. Acta. 42 (1968) 239–245.
[73] C. Sholto-Douglas-Vernon, J. Sandy, T.C. Victor, E. Sim, P.D. Helden, J. Med. Microbiol. 54 (2005) 1189–1197.